

Coupled atmosphere–ocean data assimilation experiments with a low-order model and CMIP5 model data

Robert Tardif · Gregory J. Hakim · Chris Snyder

Received: 30 June 2014 / Accepted: 20 October 2014 / Published online: 25 November 2014
© The Author(s) 2014. This article is published with open access at Springerlink.com

Abstract Coupled atmosphere–ocean data assimilation (DA) experiments are performed for estimating the Atlantic meridional overturning circulation (AMOC). Recovery of the AMOC with an ensemble Kalman filter is assessed for a range of experiments over observation availability (atmosphere, upper and deep ocean) and for assimilating high-frequency observations compared to time averages. For an idealised low-order coupled climate model, the traditional DA approach using an ensemble of model trajectories to estimate covariances is compared to a simplified “no-cycling” approach involving climatological covariances derived from a single long model integration. Robustness of the no-cycling method is also tested on data from a millennial-scale simulation of a comprehensive coupled atmosphere–ocean climate model. Results show that the no-cycling approach provides a good approximation to the traditional approach, and that assimilation of time-averaged observations improves AMOC recovery using drastically smaller ensembles than would be required for the case of instantaneous observations. Even in the limit of no ocean observations, the no-cycling approach is capable of recovering the low-frequency AMOC with time-averaged observations; assimilation of noisy instantaneous atmospheric observations fails to recover decadal-scale AMOC variability.

Keywords Cost-effective · Coupled atmosphere–ocean data assimilation · Atlantic meridional overturning circulation · Estimation

1 Introduction

Considerable research is currently devoted to improving near-term (i.e. interannual to interdecadal) climate predictions using coupled atmosphere–ocean climate models (e.g., Meehl et al. 2014). One essential aspect is the initialisation of such predictions using available observations to provide more accurate representations of phases in atmospheric and oceanic states associated with internal variability of the coupled system. Using initialised states generally results in more skillful predictions, e.g. see Troccoli and Palmer (2007), Keenlyside et al. (2008), Pohlmann et al. (2009), Mochizuki et al. (2010), Matei et al. (2012), Meehl and Teng (2012), Robson et al. (2012), Doblus-Reyes et al. (2013), Smith et al. (2013) among others. However, a lack of consensus on the most effective initialization strategies is apparent in the wide variety of approaches, particularly with respect to initialisation of low-frequency components of the climate system. Here we address this problem by considering coupled atmosphere–ocean ensemble data assimilation strategies and, in particular, conditions for which the Atlantic meridional overturning circulation (AMOC) may be recovered from a limited set of observations, including the case where only the atmosphere is observed.

Extant initialisation methods include forcing an ocean model with analysed surface fields (e.g. atmospheric and/or sea surface temperature) (e.g., Keenlyside et al. 2008; Meehl and Teng 2012; Yeager et al. 2012; Pohlmann et al. 2013); performing data assimilation (DA) in the ocean

R. Tardif (✉) · G. J. Hakim
Department of Atmospheric Sciences, University of Washington,
Box 351640, Seattle, WA 98195-1640, USA
e-mail: rtardif@atmos.washington.edu

C. Snyder
National Center for Atmospheric Research, Boulder, CO, USA

only; considering only sea surface fields (e.g., Swingedouw et al. 2013; Meinville et al. 2013); including deeper ocean observations (e.g., Tatebe et al. 2012); using weakly coupled (i.e. assimilating observations separately in the atmosphere and ocean but using a fully coupled model as a forward propagator) (e.g., Troccoli and Palmer 2007; Pohlmann et al. 2009; Mochizuki et al. 2010; Doblus-Reyes et al. 2011; Robson et al. 2012; Hazeleger et al. 2013; Ham et al. 2014); and fully coupled atmosphere–ocean DA systems (e.g., Zhang et al. 2007; Sugiura et al. 2008; Mochizuki et al. 2009; Yang et al. 2013). The latter is the most comprehensive approach as it explicitly considers covariability in atmospheric and oceanic states as part of the DA process (i.e. assimilating atmospheric observations not only generates updated atmospheric states but also updates oceanic states, and similarly for oceanic observations versus atmospheric states). The latter framework also provides the means for generating mutually consistent initial conditions (ICs) between the two coupled media, which should lead to relatively smaller initial transients in forecasts.

Despite the comprehensive nature of the fully coupled DA approach, obstacles remain to the generation of consistent coupled ICs. A key problem concerns accurate estimation of error covariances between atmospheric and oceanic states across widely different time scales. This issue has been the focus of recent studies involving the use of ensemble DA applied to simplified coupled models. Han et al. (2013) show enhanced skill in analyses of pycnocline depth through fully coupled DA, and emphasise the critical importance of using a large ensemble to adequately estimate the atmosphere–ocean cross covariances. Tardif et al. (2014) used ensemble DA applied to a low-order representation of the atmosphere coupled to a slowly overturning ocean to show that assimilating time-averaged observations increases covariability between low-frequency atmosphere–ocean interactions. Compared to the very weak covariabilities between the fast (i.e. noisy) atmosphere and slow ocean at the short time scales (i.e. frequency of observation availability), time averaging yields more robust estimates of atmosphere–ocean cross covariances with smaller ensemble size, leading to more effective coupled DA and more accurate analyses of low-frequency phases in the coupled system. The study also highlights the significant advantage of fully coupled DA in producing analyses of the AMOC, a key driver of low frequency variability.

Here we consider AMOC analysis as a canonical problem in coupled atmosphere–ocean state estimation. Proper initialisation of the AMOC is important as it is linked to enhanced predictability of North Atlantic climate (e.g., Latif and Keenlyside 2011; Boer 2011; Srokocz et al. 2012; Swingedouw et al. 2013). Despite the recent deployment of Argo profiling floats (Roemmich et al. 2009) and the Rapid

Climate Change Programme (RAPID) array, the latter specifically designed to monitor AMOC variability (Cunningham et al. 2007), and advances in assimilating these newly available observations (e.g., Smith et al. 2010; Stepanov et al. 2012; Hermanson et al. 2014), difficulties in accurately initialising the AMOC remain. These are particularly severe in the absence of comprehensive oceanic observations (e.g. Zhang et al. 2010), limiting the ability to generate realistic ICs for multidecadal hindcasts for evaluation using modern-era observations. Here, we build upon Tardif et al. (2014) (hereafter referred to as THS14) by pursuing two specific objectives:

1. Evaluate the potential of using a simplified ensemble DA approach that does not require ensemble model simulations, which we will call “no-cycling”.
2. Assess the assimilation of time-averaged observations for generating analyses of the unobserved AMOC by applying the method to a comprehensive model of the coupled atmosphere–ocean system.

The remainder of the article is organised as follows. The no-cycling DA method is described in Sect. 2. Section 3 compares AMOC analyses obtained through a traditional “cycling” approach with the no-cycling approach for experiments with the low-order coupled model described in Roeber (1995) and THS14. The impact of assimilating time-averaged observations is investigated in Sect. 4 with no-cycling experiments based on data from a simulation performed with a state-of-the-art coupled atmosphere–ocean global climate model (AOGCM) as part of the Coupled Model Intercomparison Project Phase 5 (CMIP5) (Taylor et al. 2012). A summary and conclusions are given in Sect. 5.

2 Data assimilation method

2.1 Ensemble Kalman filter

Data assimilation is performed with an ensemble Kalman filter (EnKF), for which the classical form of the update equation is:

$$\mathbf{x}^a = \mathbf{x}^b + \mathbf{K}[\mathbf{y} - \mathbf{y}^b]. \quad (1)$$

\mathbf{x}^b and \mathbf{x}^a are the background (prior) and analysis (posterior) state vectors respectively, containing joint representations of atmospheric and oceanic states. \mathbf{y} is the vector of observations while \mathbf{y}^b is the background state mapped to observation space, i.e. $\mathbf{y}^b = \mathcal{H}(\mathbf{x}^b)$, where \mathcal{H} is a forward operator that may be nonlinear. An EnKF implementation with serial processing of perturbed observations (Houtekamer and Mitchell 2001) is utilised, in which the Kalman gain \mathbf{K}_i involved in the assimilation of y_i , the i th component of \mathbf{y} , may be simply expressed as

$$\mathbf{K}_i = \text{cov}(\mathbf{x}^b, y_i^b) [\text{var}(y_i^b) + R_i]^{-1}, \quad (2)$$

where “ $\text{cov}()$ ” and “ $\text{var}()$ ” are the covariance and variance derived from ensemble estimates and therefore subject to sampling error as discussed later. Here, R_i is a scalar representing the corresponding observation error variance. Since \mathbf{x}^b is a vector containing both atmospheric and oceanic states, $\text{cov}(\mathbf{x}^b, y_i^b)$ contains covariances between variables residing in different components (i.e. atmosphere–ocean cross covariances). We note that covariance localization is not required in the context of the simplified low-dimensional system considered in this study.

2.2 Assimilation of time-averaged observations

As shown in THS14, analyses of the slowly-varying ocean can be more effectively produced through the assimilation of observations time-averaged over annual and longer intervals. Time averaging has also been considered by Sugiyama et al. (2008) in a coupled 4D-var system for the generation of enhanced predictions of seasonal to interannual variability.

With an EnKF, the update is performed using Eq. (1) with the observations and the prior replaced by their time averages, \bar{y} and $\bar{\mathbf{x}}^b$ respectively, where $\bar{(\)}$ indicates a time average. A time-invariant \mathcal{H} is assumed. The gain matrix is composed of covariances between time-averaged quantities, yielding an updated time-averaged state (i.e. $\bar{\mathbf{x}}^a$). Assuming that deviations from the time mean do not covary with time-averaged observations (i.e. $\text{cov}(\mathbf{x}^{b'}, \bar{\mathbf{y}}^b) \approx 0$, where (\prime) is a deviation from the time mean), $\mathbf{x}^{b'}$ is not changed by the assimilation and can simply be added to the updated time average to recover the full state (i.e. $\mathbf{x}^a = \bar{\mathbf{x}}^a + \mathbf{x}^{b'}$). For a more complete derivation, see Dirren and Hakim (2005) and Huntley and Hakim (2010).

2.3 The no-cycling implementation

In a traditional implementation of the EnKF, the prior is determined by the forward integration of a nonlinear model from past analysed ensemble states. The information provided by assimilating observations is thus carried by the model from one DA update to the next (i.e. cycling). In the context of near-term coupled atmosphere–ocean predictions, this approach requires that an ensemble of AOGCM simulations be carried out, which demands considerable computer resources.

A simplification consists of foregoing the forward integration of ensemble members in favor of using model states drawn from a single model integration. Specifically, the \mathbf{x}^b ensemble is formed using N random draws of model states from a preexisting, preferably long, coupled simulation, where N is the ensemble size. This is done at every DA

update time, hence forecasts from a previous analysis are not used (i.e. DA without cycling). In the limit of large N , the prior ensemble-mean corresponds to the model’s climatology and deviations from the mean represent anomalies. If, in addition, the model approximately reproduces the observed climatology, the ensemble will be drawn from the same distribution as the true state to be estimated and covariance inflation will not be required (see Huntley and Hakim 2010).

With this simplified approach, ensemble-estimated error covariances now represent climatological statistics (i.e. no longer time- or flow-dependent). The use of climatological error covariances estimated from a single long model integration as an inexpensive alternative was first proposed by Oke et al. (2002) and described as the ensemble optimal interpolation (EnOI) approach by Evensen (2003). Although there is evidence that the EnKF outperforms EnOI (e.g. Oke et al. 2007), the more cost effective approach has been shown to be a viable alternative in a number of applications (e.g. Oke et al. 2005).

Steiger et al. (2014) successfully use time averages in a no-cycling approach for paleoclimate reconstructions. However, the adverse consequences, if any, from the use of climatological rather than flow-dependent error statistics and absence of cycling remain unknown in a context of fully coupled atmosphere–ocean state estimation. The impact of these simplifications is estimated in Sect. 3 with the simple coupled model used in THS14.

3 Efficient DA with a low-order coupled model

The model is an idealised simplification of the North Atlantic climate system, with a large-scale atmospheric circulation (Lorenz 1984) interacting with a Stommel 3-box model of the meridionally overturning ocean (Stommel 1961). In this “Lorenz–Stommel” coupled model, high-frequency atmospheric variability is driven by interactions between the zonal jet and transient eddies, both influenced by low-frequency variability of the upper ocean temperature. Low-frequency variability in ocean temperature and salinity is driven by nonlinear interactions with the thermohaline overturning circulation. In turn, the atmosphere influences the overturning circulation by modulating the meridional gradient of upper ocean salinity through a simple representation of the hydrological cycle (i.e. evaporation over subtropical waters, eddy-driven poleward transport of water vapor and freshening of the subpolar ocean by precipitation). For a more comprehensive description of the Lorenz–Stommel coupled model see Roebber (1995) and THS14.

THS14 compare analyses of the unobserved AMOC generated using coupled ensemble DA (EnKF) performed

on a daily basis (i.e. defined as the frequency of observation availability) against analyses obtained from the assimilation of time-averaged (i.e. yearly) observations. This is motivated by the increase of the atmosphere-AMOC covariability in the model for time scales longer than one year. Similar experiments are carried out here, but for the no-cycling implementation of the EnKF. As before, a perfect model framework is used, with truth and observations taken from the same 5,000-year-long reference simulation described in THS14, along with the same observation error statistics (10 % of climatological standard-deviations for atmospheric variables and 0.5 K for ocean temperature and 0.1 psu for salinity).

3.1 Sampling error and ensemble size

To gauge the necessary ensemble size, AMOC analyses are produced using no-cycling DA with ensemble sizes varying from 5 to 5,000 for daily atmospheric observations. This scenario represents the most severe test for ensemble covariance estimation as atmosphere-AMOC covariances are very weak at the daily time scale (see THS14). For each ensemble size, analyses are generated over one hundred randomly sampled 5-year periods from the reference simulation in order to sample a wide variety of climate states. The root-mean-square error (RMSE) over the one hundred realisations is shown as a function of ensemble size in Fig. 1. As expected, RMSE values are largest for the smaller ensembles, and rapidly decrease with an increase in ensemble size. A plateau is reached for ensembles of about 500 members, beyond which average RMSE values continue to decrease, but at a smaller rate. This value represents a lower bound for robust estimation of climatological covariances

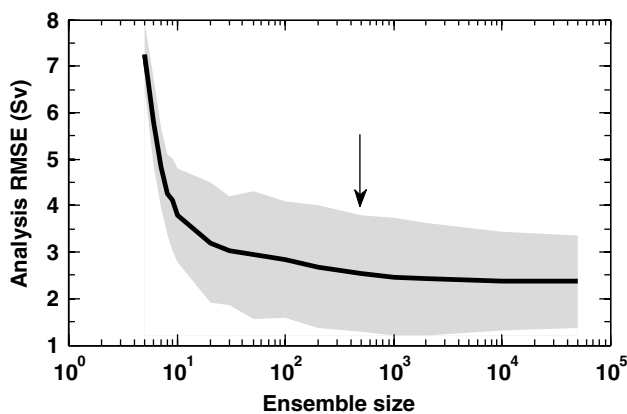


Fig. 1 Root mean square error (RMSE) of AMOC analyses in Sverdrups (Sv) obtained from no cycling atmosphere-only daily DA experiments using various ensemble sizes. The *solid line* represents average RMSE values compiled over 100 realizations of each set of year-long DA experiments (i.e. each ensemble size) while the shaded area indicates 90 % confidence intervals. The *arrow* indicates the ensemble size chosen for the DA experiments

between instantaneous atmosphere and ocean states in the simple model, and is used for the no-cycling experiments presented next.

3.2 Cycling–no-cycling comparison

AMOC analyses generated using climatological information for the prior ensemble are compared to a traditional DA configuration with cycling of model ensembles. At every analysis time, the prior is defined using 500 random draws of daily model states from the reference solution and analyses covering the first 1,000 years of the reference simulation are produced, a period long enough to sample the various phases of the ocean’s low-frequency variability. Distinct sets of analyses are produced in which progressively fewer oceanic variables are assimilated:

- Temperature and salinity in the subtropical and sub-polar upper ocean, and in the deep ocean (i.e. well-observed ocean),
- Temperature and salinity in the upper ocean only,
- Upper ocean temperature only,
- None (i.e. only atmospheric observations).

Experiments also consider different variables describing transient eddies in the atmosphere, i.e. eddy phases and eddy energy, the latter being characterised by a significantly enhanced covariability with the AMOC when states are time-averaged over annual and longer time scales (see THS14 Fig. 6).

The accuracy of analyses is evaluated using the coefficient of efficiency (Nash and Sutcliffe 1970):

$$CE = 1 - \frac{\sum_{i=1}^M (x_i^t - x_i^a)^2}{\sum_{i=1}^M (x_i^t - \bar{x}^t)^2}, \quad (3)$$

where x_i^t is the truth at time t_i and \bar{x}^t is the corresponding time mean, while x_i^a are the analyses. CE is a relative measure of the analysis error variance to the variance in true states. This is a particularly attractive feature in a context of examining skill at various temporal scales, as averaging over longer time intervals leads to reduced variances in the signal. Perfect analyses have $CE = 1$ while $CE \approx 0$ characterises analyses that do not contain additional information over climatology.

Results for cycling DA show that more accurate AMOC analyses are obtained when observations are assimilated in the ocean (Fig. 2). The loss of accuracy associated with fewer assimilated oceanic observations is reduced for time-averaged observations, particularly for atmospheric eddy energy observations. There is no skill for daily DA of only

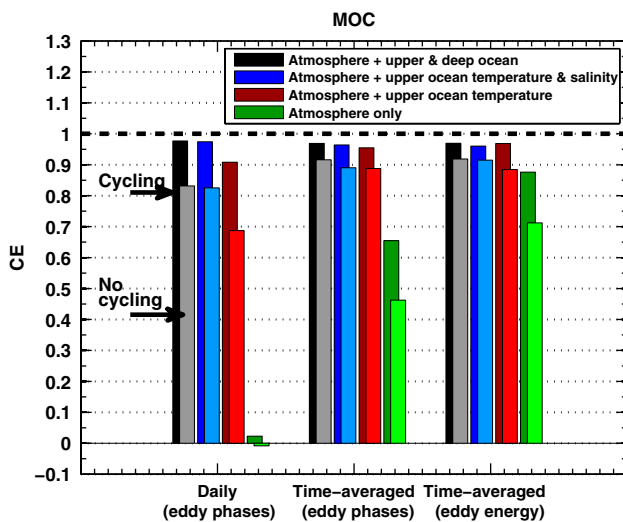


Fig. 2 Coefficient of efficiency (CE) characterising AMOC analyses from the low-order coupled model obtained with the various DA configurations considered. Results obtained with cycling the model are shown using *darker colors* and the corresponding no-cycling results are shown using *lighter colors*

atmospheric observations, whereas the reduction in skill between assimilating ocean observations compared to only atmospheric observations is of the order of 20 % when individual time-averaged eddy phases are assimilated and only 10 % when eddy energy is assimilated. By comparison, no-cycling daily DA is found to be less accurate by 15–25 % when ocean observations are assimilated, while the assimilation of only atmospheric variables still has no skill. In contrast, the decrease in accuracy between cycling and no-cycling is only 5–10 % for yearly time-averaged DA when oceanic observations are assimilated, and 30 % with only-atmosphere observations. When time-averaged observations of eddy energy are assimilated instead of the individual eddy phases, the decrease in skill is only about 5–10 % with ocean DA, and 20 % in the only-atmospheric case.

These results suggest that no-cycling DA is a viable alternative to the more computationally intensive cycling DA. A decrease in skill is evident, but by a reduced margin when time-averaged observations are assimilated.

4 Experiments with CMIP5 data

Motivated by the results for the idealised model, we next repeat, as closely as possible, the previous no-cycling experiments using gridded simulation data from a comprehensive AOGCM.

A perfect model framework is adopted for DA experiments using data from the “Last Millenium” simulation of

the Community Climate System Model Version 4 (CCSM4) (Gent et al. 2011) performed in the context of the Coupled Model Intercomparison Program Phase 5 (CMIP5) (Taylor et al. 2012). This simulation and model were chosen as they represent the longest available pre-industrial simulation (i.e. covering the period from 850 to 1,850) from a well-characterised coupled climate model. The simulation constitutes a state-of-the-art depiction of climate’s natural variability, externally influenced by solar activity and variability in aerosols from volcanic eruptions. No anthropogenically induced trends in greenhouse gas concentrations are imposed. To preserve a basis for comparison with results presented above, gridded model output is “coarse-grained” to a set of variables similar to those in the Lorenz–Stommel model.

4.1 Low-order variables

The CMIP5 database contains monthly-averaged data for a wide variety of variables, including the AMOC streamfunction for certain models and experiments, while daily data is available for a restricted set of model output. Hence, the monthly time scale is considered as the shortest represented scale in the low-order analogue, and defines the frequency at which observations are available.

The Atlantic basin north of the equator is divided into three boxes as in the Lorenz–Stommel model, with an upper ocean subtropical box defined from the equator to 40°N, an upper ocean subpolar box between 40°N to 65°N. The deep ocean is represented by a box covering the equator to 65°N. Monthly temperature and salinity data at a depth of 200 m are taken as representative of the upper ocean and are spatially averaged over the respective boxes. Data at 2 km depth, averaged over the whole basin, are taken as representing the deep ocean.

For the atmosphere, gridded monthly-averaged 700 hPa air temperatures are spatially averaged over subtropical and subpolar boxes respectively, defined using the same latitude-longitude boundaries as in the ocean. A mean westerly circulation component (i.e. zonal wind) is derived by taking the temperature difference between the subtropical and subpolar boxes (i.e. thermal wind balance) so that positive values indicate westerlies. Similar area-averaged tropospheric humidity variables are derived using gridded 700 hPa specific humidity data. Variables describing transient atmospheric eddies are defined by an approach similar to Chang et al. (2013). First, daily mean sea-level pressure data are used to derive the variance of pressure perturbations associated with transient eddies (i.e. eddy variance) at every grid point using the 24-hr filter of Wallace et al. (1988):

$$E = \overline{(P_{mst})^2} = \overline{[P_{mst}(t + 24hr) - P_{mst}(t)]^2}, \quad (4)$$

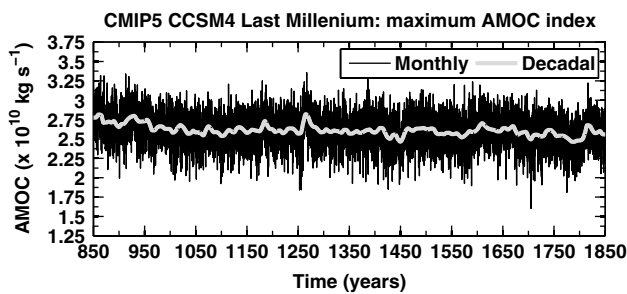


Fig. 3 Temporal evolution of the maximum value of meridional overturning streamfunction in the last-millennium simulation of CCSM4. Monthly averaged (solid black line) and 10-year averaged (solid gray line) values are shown

where P_{msl} is the daily mean sea-level pressure and t represents time. The overbar in (4) represents a monthly average. As pointed out by Chang et al. (2013) this simple 24-hour difference filter has a response highlighting the synoptic time scale, i.e. transient eddies. Gridded meridional eddy heat and water vapor fluxes are similarly estimated using the following covariances:

$$H_E = \overline{v'_g T'} = \overline{(v_g(t + 24hr) - v_g(t))(T(t + 24hr) - T(t))}, \quad (5a)$$

$$M_E = \overline{v'_g q'} = \overline{(v_g(t + 24hr) - v_g(t))(q(t + 24hr) - q(t))}, \quad (5b)$$

where v_g is the daily surface meridional geostrophic wind derived from mean sea level pressure and T and q are the daily near-surface air temperature and specific humidity respectively. Low-order variables are then formulated by averaging the gridded values of eddy amplitude and eddy heat and moisture fluxes along the 40°N transect across the Atlantic Ocean.

Finally, a single variable describing the time-varying strength of the overturning circulation is derived by taking the maximum monthly value of the AMOC streamfunction within a latitude-depth cross-section between 30°N and 70°N and between depths of 500 m and 2000 m as in Zhang et al. (2010) and Danabasoglu et al. (2012).

4.2 AMOC variability and covariability

The time series of maximum AMOC streamfunction in the North Atlantic (i.e AMOC index) from the 1,000-year CCSM4 simulation is shown in Fig. 3. The maximum transport is characterised by an average value $2.6 \times 10^{10} \text{ kg s}^{-1}$ and rich variability, e.g. substantial seasonal and interannual variations superimposed on low-frequency variability characterised by well-defined periods of enhanced poleward transport as evidenced by the 10 year moving average. Here, the main focus is on recovering the low-frequency component of the AMOC.

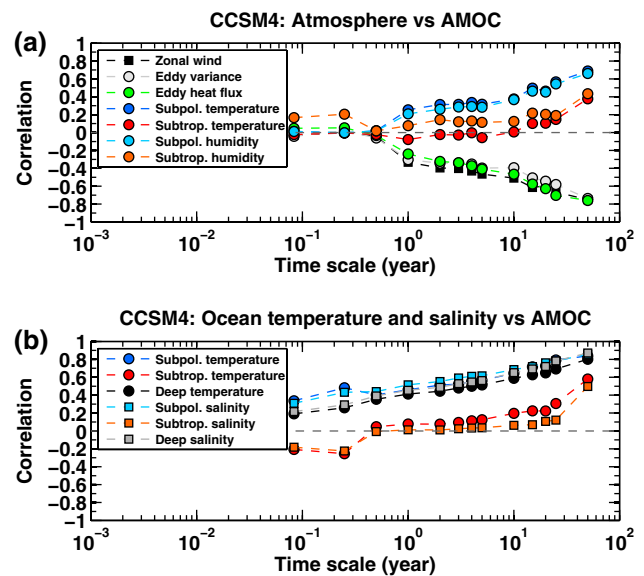


Fig. 4 Correlations between atmospheric (upper frame) and oceanic (lower frame) low-order variables representing subpolar (high-latitude) and subtropical (low-latitude) and the maximum AMOC index, for various averaging time scales, in the CCSM4 Last Millennium CMIP5 simulation

The correlations between the AMOC maximum transport and each of the low-order variables described in the previous section are shown as a function of averaging time scale in Fig. 4. As in the low-order model, covariability between the AMOC and the atmosphere is weak at sub-annual time scales. Only a slight increase toward positive correlations takes place in the 1–10 year range for variables describing the mean subpolar atmosphere, while covariability with the subtropical atmosphere remains weak. A small increase in correlation is evident for averaging time intervals longer than a decade. The mean westerly circulation (i.e. temperature difference between the subtropical and subpolar atmosphere) is negatively correlated with the AMOC at interannual time scales and longer, with an increasing correlation magnitude for longer averaging time scales. This suggests that a stronger AMOC is associated with a warmer subpolar atmosphere, but with a weaker effect on the subtropical atmosphere resulting in a reduction in the tropospheric meridional temperature gradient and weaker westerlies.

Similar behavior is observed for variables related to atmospheric eddies, with negative correlations increasing in magnitude for averaging intervals of one year and longer. This is consistent with the “Bjerknes compensation” mechanism (Bjerknes 1964), which posits that under weakly varying top-of-atmosphere radiative fluxes and heat storage, the total energy transport should not vary greatly, implying compensating responses in large-scale heat transport between the ocean and atmosphere. Shaffrey and Sutton

(2006) analysed output from a control run of the Third Hadley Centre Coupled Ocean Atmosphere General Circulation Model (HadCM3) and found that a stronger AMOC and related poleward heat transport lead to reduced large-scale baroclinicity in the atmosphere, which in turn leads to a weakened transient eddy transport. These authors also found that the degree of compensation in the northern extratropics increases with increasing time scale as found here. Farnetti and Vallis (2013) also found a significant degree of compensation between atmospheric and oceanic meridional fluxes at decadal time scales in two different models developed at the Geophysical Fluid Dynamics Laboratory (GFDL). They also found positively correlated moisture and sensible heat transport, as diagnosed here in the CCSM4 (e.g. although the moisture eddy flux is not shown in Fig. 4a, both eddy fluxes are similarly anticorrelated with the AMOC). These results suggest that significant consistencies exist in decadal-scale atmosphere–AMOC interactions between the CCSM4 and other state-of-the-art AOGCMs (e.g. HadCM3 and GFDL models).

Clear signals are also present in the ocean (Fig. 4b). Correlations between the AMOC index and subpolar upper ocean temperature and salinity are weakly positive at the monthly time scale, and gradually increase with the averaging interval, to values greater than 0.8 for 50-year time averages. Strong decadal-scale covariability between the AMOC and upper ocean temperature over large areas of the subpolar Atlantic have already been reported in the CCSM4 (Danabasoglu et al. 2012) and in various other models (e.g., Latif et al. 2004; Knight et al. 2005; Heslop and Paul 2012; Cheng et al. 2013; Roberts et al. 2013). The positive correlation between the AMOC and upper subpolar ocean salinity in CCSM4 described here is also consistent with other models (e.g., Cheng et al. 2013).

Covariability with the subtropical ocean is weakly negative at sub-annual time scales, becoming very weak in the interannual to decadal range, and increasing to larger positive values for averaging intervals longer than a decade. Deep ocean temperature and salinity are positively correlated with the AMOC index, with correlation strength increasing with averaging time scales. Corroboration with other research is less clear in this case. Wang and Zhang (2013) describe intricate AMOC-related anticorrelated variability between the upper and deeper temperature at subtropical latitudes in “historical” simulations covering the industrial period. Such regional signals are lost when averaging over large regions as we do here. Nevertheless, Wang and Zhang (2013) find a positive regression between AMOC-driven decadal-scale upper ocean temperature variations and basin-wide temperature to depths of 2 km in some models, including the CCSM4, consistent with our results. Significant differences are apparent in how the upper and deep ocean are connected in various models,

suggesting large uncertainties remain in the attribution and simulation of mechanisms determining the statistical links described above.

The details of the causal relationships between the AMOC and other state variables is beyond the scope of this work. From a DA perspective, the covariability characteristics are most important, particularly their dependence on time scale. Experiments designed to explore how this covariability can be exploited for improved coupled DA are presented next.

4.3 Data assimilation experiments

The system is composed of time series of the coarse-grained variables, forming the basis for DA experiments in a perfect-model framework. Synthetic observations are constructed by starting with the monthly averaged states from the 1,000-year simulation, excluding the AMOC index, and adding independent realizations of Gaussian noise whose standard deviation is taken as 10 % of the climatological value. As in THS14, error statistics of time-averaged observations are appropriately scaled by reducing the standard deviation by a factor equal to the square root of the number of observations used to calculate the average. Analyses of the AMOC index are produced for monthly observations and compared to those derived from time-averaged observations with averaging intervals of 1, 5, 10, 25 and 50 years.

As in THS14, two configurations of assimilated atmospheric variables are considered. A basic DA configuration includes the assimilation of zonal wind, eddy variance, tropospheric air temperature and specific humidity (subtropical, subpolar). A second configuration is tested, in which the eddy variance and tropospheric temperatures and humidities are replaced by the meridional eddy fluxes of heat and water vapor, akin to tests performed in THS14 with the assimilation of eddy energy, a higher-order variable correlating more strongly with the AMOC.

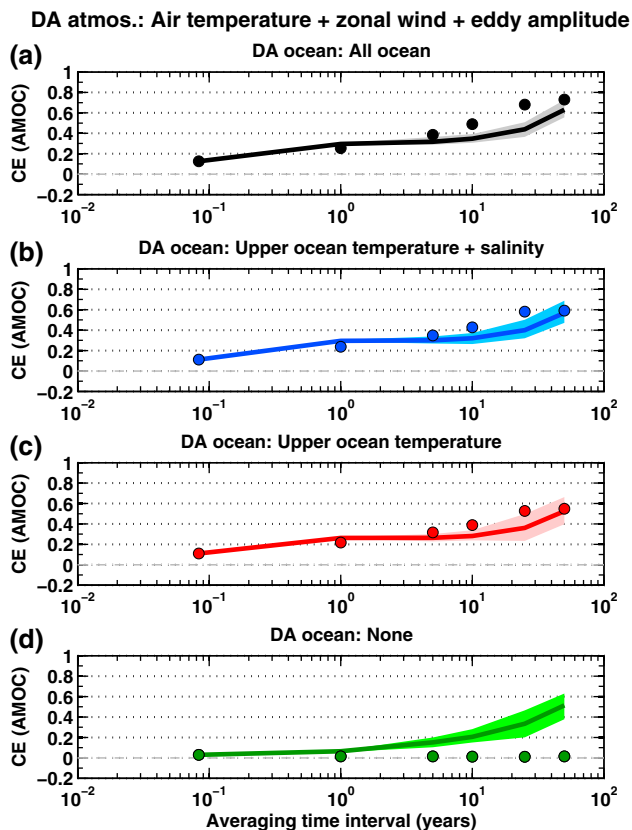
Ensemble size should be large enough to minimize sampling error but is limited by the availability of independent samples in the finite-length reference simulation. In a noisy system with memory (i.e. red noise spectra), as in the coupled atmosphere–ocean system, we follow Bretherton et al. (1999) who show that for quadratic statistics between two variables x_1 and x_2 , an estimate of the number of independent samples is

$$N_{ind} = N_{tot} \frac{1 - r_1 r_2}{1 + r_1 r_2}, \quad (6)$$

where N_{tot} is the total number of available samples and r_1 and r_2 are the respective lag-1 autocorrelation coefficients. This estimate is applied to time series of the AMOC and the other variables time-averaged over the various intervals considered. Corresponding estimates of independent

Table 1 Ensemble sizes (i.e. number of independent samples) used in the CMIP5 data assimilation experiments

Averaging interval	Ensemble size
Month	5,000
1 year	300
5 years	70
10 years	50
25 years	20
50 years	15

**Fig. 5** Coefficient of efficiency (CE) of AMOC analyses produced with the baseline DA configuration, for various levels of assimilated oceanic observations: **a** all, **b** upper ocean temperature and salinity, **c** upper ocean temperature only, **d** no ocean observations. *Solid lines* correspond to the average and *shaded areas* indicating the 10th and 90th percentiles of the CE distribution from one hundred realisations of each experiment with the assimilation of time-averaged observations. *Dots* represent the average CE for monthly AMOC analyses time-averaged over corresponding time intervals

samples (i.e. ensemble sizes used in DA experiments) are shown in Table 1. Ensemble sizes decrease to relatively small numbers for longer averaging intervals, but any adverse impact is compensated by the stronger covariabilities between key state variables and the AMOC over these longer scales. This reduces the need for large ensembles

for reliable estimation of covariances. Monte Carlo experiments indicate that statistical significance levels of estimated covariances can be maintained at 90 % using ensemble sizes listed in Table 1, except for variables defining subtropical states (not shown). The remaining impact of sampling error on the analyses is discussed below.

A series of DA experiments are performed for contrasting scenarios of observation availability, including the extreme case of atmosphere-only observations. For each time-averaging interval, and observation-availability scenario, one hundred sets of analyses covering the entire Last Millennium simulation are produced. The ability to recover the AMOC using the different DA configurations is summarised in Figs. 5 and 6. Note that CE values corresponding to the ensemble-mean background states are zero, including those for time-averaged states. Here, the ensemble-mean represents the model climatology, without any specific information about states taken at any particular time. The departure from zero for CE values characterising analysed states can be considered a measure of the information gained through DA.

Time-averaged AMOC analyses CE values increase with averaging time, indicating relatively more accurate analyses with respect to climatology. Not surprisingly, results slightly deteriorate as fewer oceanic observations are assimilated. The assimilation of atmospheric meridional heat flux leads to more accurate time-averaged AMOC analyses compared to eddy amplitude, particularly for decadal and longer time averages. This contrast is greatest for the atmosphere-only case.

The impact of sampling errors on AMOC analyses, represented by the spread in CE distribution (see shaded areas in Figs. 5, 6), is small for averages less than 10 years but increases for longer times scales. In comparison to the larger ensembles used for the shorter time scales, the smaller ensembles associated with averages over the longer intervals lead to a slight increase in sampling uncertainty. Such uncertainty in AMOC analyses decreases for atmospheric eddy flux assimilation due to enhanced covariability with that quantity.

For reference, results corresponding to the monthly AMOC analyses “upscaled” (i.e. time averaged) to the different intervals are shown as dots on Figs. 5 and 6. CE values for time-averaged DA that exceed the upscaled monthly analyses indicate added value from assimilating time-averaged observations. Upscaled monthly analyses are of superior accuracy when ocean observations are assimilated for interannual and longer time averages when the baseline DA configuration is used; this difference decreases when eddy heat flux is assimilated. The most noticeable advantage of time-averaged DA is obtained for atmosphere-only assimilation, which is dramatic for multidecadal time averages. In this case, monthly analyses have no skill at representing the

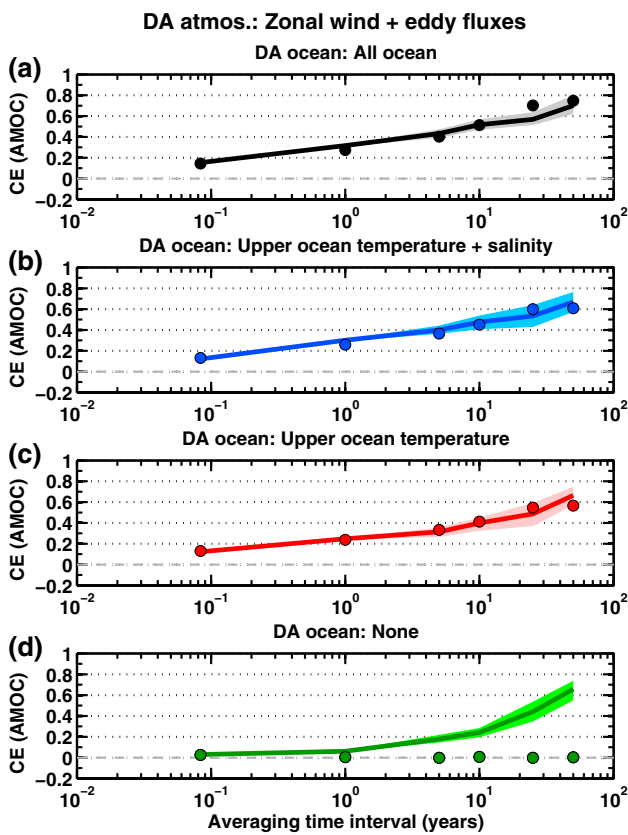


Fig. 6 Same as Fig. 5 but for the configuration assimilating eddy fluxes in the atmosphere

low frequency AMOC variability, whereas AMOC analyses obtained from the assimilation of time-averaged atmospheric observations are only slightly less accurate than those obtained with ocean DA.

To assess the level of skill in recovering non-assimilated oceanic variables other than the AMOC, CE values for analysed ocean temperature and salinity are evaluated for the case where atmospheric eddy fluxes are observed. Results for the subpolar upper ocean are shown (Figs. 7 and 8 for temperature and salinity respectively), as well as for the subtropical upper and deep ocean temperature (Figs. 9 and 10). Similar results are found for deep ocean salinity (not shown). These figures only show results for analysis variables that are not assimilated. Analyses of assimilated variables give CE values near unity as expected (not shown). Results confirm the lack of skill at representing consistent oceanic states when performing monthly DA with atmospheric observations only. Corresponding CE values remain near zero even when analyses are averaged over longer time scales; the information on ocean low-frequency variability contained in monthly atmospheric fields is hidden beneath the noise characterising the subannual variability of the atmosphere.

However, analyses of the subpolar upper ocean from atmosphere-only DA (Figs. 7, 8b) show enhanced skill

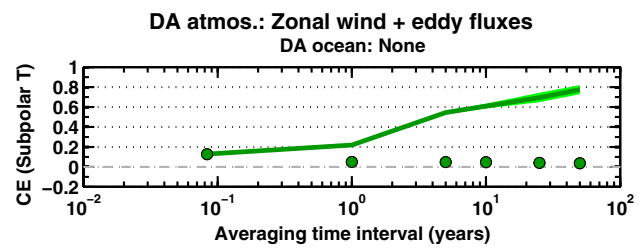


Fig. 7 Coefficient of efficiency (CE) for analyses of the subpolar upper ocean temperature in experiments with assimilation of atmospheric data only (i.e. the only DA configuration for which this variable is not assimilated in our experiments)

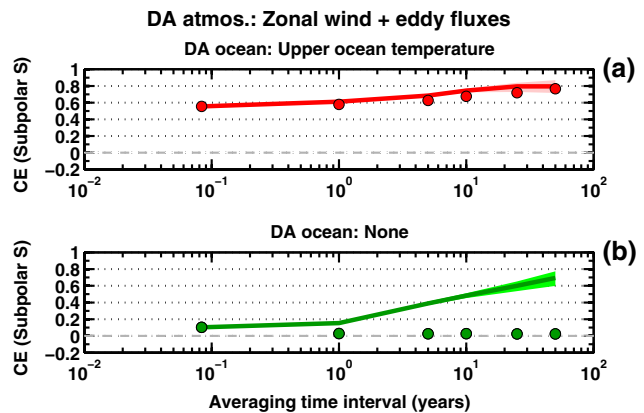


Fig. 8 Coefficient of efficiency (CE) for analyses of the subpolar upper ocean salinity in experiments with assimilation of **a** atmospheric observations and upper ocean temperature and **b** atmospheric data only (i.e. only DA configurations for which the considered variable is not assimilated)

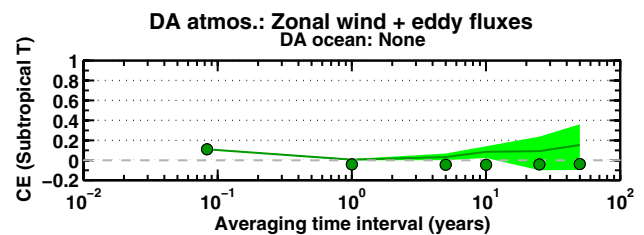


Fig. 9 Coefficient of efficiency (CE) for analyses of the subtropical upper ocean temperature in experiments with assimilation of atmospheric data only

when time-averaged observations are assimilated, particularly for longer time averages. More accurate salinity analyses are obtained when upper ocean temperature observations are assimilated (Fig. 8a) compared to when DA is performed in the atmosphere only (Fig. 8b), confirming the importance of temperature–salinity covariability (e.g., Zhang et al. 2007). Furthermore, comparable accuracy is obtained with time-averaged DA compared to upscaling monthly analyses (i.e. solid lines versus dots in Fig. 8a).

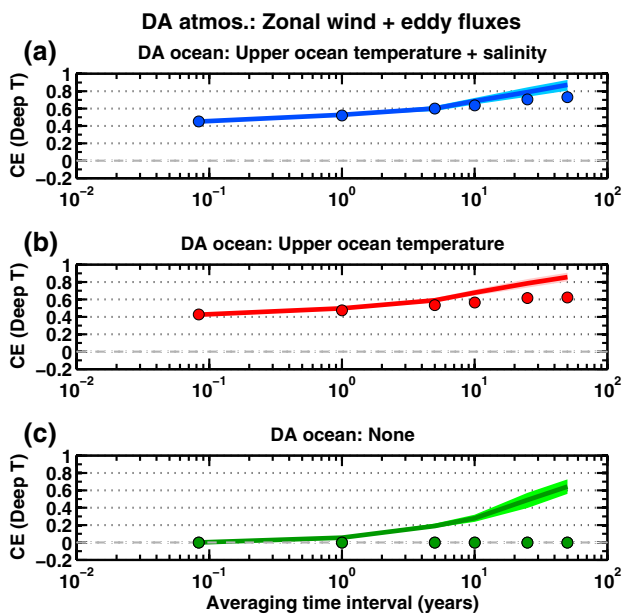


Fig. 10 Coefficient of efficiency (CE) for analyses of the deep ocean temperature in experiments with assimilation of **a** atmospheric observations and upper ocean temperature and salinity, **b** atmospheric observations and upper ocean temperature and **c** atmospheric data only

For the subtropical upper ocean, temperature analyses show no skill in the case of atmosphere-only observations, for both monthly and time-averaged DA (Fig. 9). As with subpolar salinity, more skillful analyses are obtained at all time scales when observations of upper ocean temperature are assimilated (not shown).

Deep-ocean temperature is recovered with similar accuracy on subdecadal timescales for both monthly and time-averaged upper oceanic observations, while slightly more skillful analyses of low frequency variability (i.e. decade and longer) are obtained with time-averaged DA (Fig. 10a, b). The advantage of time-averaged DA is again apparent for the atmosphere-only case (Fig. 10c), particularly at the longest averaging time scale considered where the skill is similar to the case where upper ocean observations are assimilated. Although not shown, we find similar skill in analyses of deep ocean salinity.

5 Summary and conclusions

We have examined coupled atmosphere–ocean data assimilation (DA) techniques with an emphasis on analysing the low-frequency AMOC. Our study is motivated by the need for computationally efficient initialization of the AMOC when limited or no ocean observations are available, and

it extends Tardif et al. (2014) who demonstrated that time averaging of observations greatly improved the AMOC analyses from an EnKF assimilating only atmospheric observations.

The “no-cycling” DA approach proposed here combines two ideas. First, we use time averages of observations as in Tardif et al. (2014) to update estimates of the slowly varying components of the atmosphere–ocean system. Second, we use an ensemble drawn from a climatological simulation of an atmosphere–ocean coupled climate model (AOGCM) as the background, hence using climatological covariance information during DA as proposed by Oke et al. (2002). No-cycling DA eliminates the need for multiple integrations of an AOGCM, but at the expense of lacking the state-dependent covariances.

We pursued two specific objectives: (1) evaluate the potential of the cost-effective no-cycling DA, in particular whether using flow-dependent covariances is crucial to initialising the AMOC and, (2) assess the value of assimilating time averages of observations in a more realistic representation of the climate system compared to the low-order model used by Tardif et al. (2014). Experiments in two different settings are performed: one with the simplified low-order model to address objective (1) and the second using synthetic observations generated from a long integration of a state-of-the-art AOGCM to address objective (2).

Results from the low-order model show that ensemble DA based on a climatological ensemble, in which members are drawn from a single long model integration, performs nearly as well as a full EnKF when estimating the AMOC from time-averaged observations. Thus, in the context of this simplified model, it is not essential to capture the temporal variation of covariances between the low-frequency AMOC and oceanic and atmospheric observables.

A powerful capability enabled by the no-cycling simplification is the straightforward evaluation of fully coupled DA with a more complex and realistic AOGCM at minimal cost. Given the results above, we performed DA experiments similar to those in the simple low-order model but using data from the “Last Millenium” simulation of the CCSM4 model. These experiments derive from a long time series of coarse-grained atmospheric and oceanic variables from the gridded model output. Synthetic observations having additive noise are assimilated to assess the potential for estimating the AMOC. As in the simple model, no-cycling DA provides useful estimates of AMOC variability at decadal scales and longer given only time-averaged atmospheric observations, because the AMOC and atmospheric observables covary strongly over time scales of several years and longer. In addition, we find that low-frequency temperature and salinity variability in other parts of the ocean (e.g., particularly the subpolar upper and basin-scale

deep ocean) can also be recovered with no-cycling DA, demonstrating the robustness of the results obtained in Tardif et al. (2014).

We acknowledge that these results are based on an assumption of a perfect model and therefore represent a best-case scenario. Larger analysis errors are expected in the more realistic case of an imperfect model, either arising from model biases or from erroneous covariances between state variables and observables. Techniques to circumvent the effect of model biases exist, such as anomaly initialisation (e.g., Carassi et al. 2014) or application of posteriori correction methods (e.g., Fučkar et al. 2014), all of which can be adapted to the concepts proposed here. The issue of errors related to misrepresented covariances however remains an open question that warrants closer attention. Such efforts are left for future endeavors.

Despite the best-case character of the results, the proposed fully coupled DA approach, combining no-cycling and time-averaging of observations, has the potential to yield accurate estimates of the low-frequency AMOC and other key ocean variables, with modest computational cost, even for time periods where availability of observations in the ocean is minimal or nonexistent. These results are relevant not only for improving our ability to efficiently produce analyses of the modern AMOC, but also for estimating the past AMOC. A crucial step in developing enhanced climate prediction capabilities is to perform decadal-scale hindcasts, whose quality can be evaluated using modern-era observations but which must be initialized at times pre-dating the deployment of a denser network of oceanic observations.

In considering the complete initial-value problem of decadal climate predictions, the findings of this study suggest that future efforts should focus on extending the proposed DA method to a multi-time scale approach and assessing its potential for initialising other subcomponents of the coupled climate system involving interactions over multiple time scales, such as the land-atmosphere system.

Acknowledgments This research was supported by the National Science Foundation grant NSF-1048834 awarded to the University of Washington. Two anonymous reviewers are thanked for their constructive comments. We acknowledge the Program for Climate Model Diagnosis and Intercomparison and the WCRP's Working Group on Coupled Modelling for their roles in making available the CMIP5 data set. Support of the CMIP5 dataset is provided by the U.S. Department of Energy (DOE) Office of Science. The National Center for Atmospheric Research is sponsored by the National Science Foundation.

Open Access This article is distributed under the terms of the Creative Commons Attribution License which permits any use, distribution, and reproduction in any medium, provided the original author(s) and the source are credited.

References

- Bjerknes J (1964) Atlantic air-sea interaction. In: Landsberg HE, van Mieghem J (eds) *Advances in geophysics*, vol 10. Academic Press, New York, pp 1–82
- Boer GJ (2011) Decadal potential predictability of twenty-first century climate. *Clim Dyn* 36:1119–1133. doi:10.1007/s00382-010-0747-9
- Bretherton CS, Widmann M, Dymnikov VP, Wallace JM, Bladé I (1999) The effective number of spatial degrees of freedom in a time-varying field. *J Clim* 12:1990–2009
- Carassi W, Weber RJT, Guémas V, Doblas-Reyes FJ, Asif M, Volpi D (2014) Full-field and anomaly initialization using a low-order climate model: a comparison and proposals for advanced formulations. *Nonlinear Process Geophys* 21:521–537. doi:10.5194/npg-21-521-2014
- Chang EKM, Guo Y, Xia X, Zheng M (2013) Storm-track activity in IPCC AR4/CMIP3 model simulations. *J Clim* 26:246–260. doi:10.1175/JCLI-D-11-00707.1
- Cheng W, Chiang JCH, Zhang D (2013) Atlantic meridional overturning circulation (AMOC) in CMIP5 models: RCP and historical simulations. *J Clim* 26:7187–7197. doi:10.1175/JCLI-D-12-00496.1
- Cunningham SA, Kanzow T, Rayner D, Baringer MO, Johns WE, Marotzke J, Longworth HR, Grant EM, Hirschi JJM, Beal LM, Meinen CS, Bryden HL (2007) Temporal variability of the Atlantic meridional overturning circulation at 26°N. *Science* 317:935–938
- Danabasoglu G, Yeager SG, Kwon YO, Tribbia JJ, Phillips AS, Hurrell JW (2012) Variability of the Atlantic meridional overturning circulation in CCSM4. *J Clim* 25:5153–5172
- Dirren S, Hakim GJ (2005) Toward the assimilation of time-averaged observations. *Geophys Res Lett* 32:L04804. doi:10.1029/2004GL021444
- Doblas-Reyes FJ, Balmaseda MA, Weisheimer A, Palmer TA (2011) Decadal climate prediction with the European Centre for Medium-Range Weather Forecasts coupled forecast system: impact of ocean observations. *J Geophys Res* 116:D19111. doi:10.1029/2010JD015394
- Doblas-Reyes FJ, Andreu-Burillo I, Chikamoto Y, García-Serrano J, Guémas V, Kimoto M, Mochizuki T, Rodríguez LRL, van Oldenborgh GJ (2013) Initialized near-term regional climate change prediction. *Nat Commun* 4:1715. doi:10.1038/ncomms2704
- Evensen G (2003) The ensemble Kalman filter: theoretical formulation and practical implementation. *Ocean Dyn* 53:343–367
- Farnetti R, Vallis GK (2013) Meridional energy transport in the coupled atmosphere–ocean system: compensation and partitioning. *J Clim* 26:7151–7166. doi:10.1175/JCLI-D-12-00133.1
- Fučkar NS, Volpi D, Guémas V, Doblas-Reyes FJ (2014) A posteriori adjustment of near-term climate predictions: accounting for the drift dependence on the initial conditions. *Geophys Res Lett* 41:5200–5207. doi:10.1002/2014GL060815
- Gent PR, Danabasoglu G, Donner LJ, Holland MM, Hunke EC, Jayne SR, Lawrence DM, Neale RB, Rasch PJ, Vertenstein M, Worley PH, Yang ZL, Zhang M (2011) The community climate system model version 4. *J Clim* 24:4973–4991
- Ham YG, Rienecker MM, Suarez MJ, Vikhliav Y, Zhao B, Marchak M, Vernières G, Schubert SD (2014) Decadal prediction skill in the GEOS-5 forecast system. *Clim Dyn* 42:1–20. doi:10.1007/s00382-013-1858-x
- Han G, Wu X, Zhang S, Liu Z, Li W (2013) Error covariance estimation for coupled data assimilation using a Lorenz atmosphere and a simple pycnocline ocean model. *J Clim* 26:10,218–10,231. doi:10.1175/JCLI-D-13-00236.1

- Hazeleger W, Wouters B, van Oldenborgh GJ, Corti S, Palmer T, Smith D, Dunstone N, Kröger J, Pohlmann H, von Storch JS (2013) Predicting multiyear North Atlantic Ocean variability. *J Geophys Res* 118:1087–1098. doi:[10.1002/jgrc.20117](https://doi.org/10.1002/jgrc.20117)
- Hermanson L, Dunstone N, Haines K, Robson J, Smith D, Sutton R (2014) A novel transport assimilation method for the Atlantic meridional overturning circulation at 26°N. *Q J R Meteor Soc*. doi:[10.1002/qj.2321](https://doi.org/10.1002/qj.2321)
- Heslop D, Paul A (2012) Fingerprinting of the Atlantic meridional overturning circulation in climate models to aid in the design of proxy investigations. *Clim Dyn* 38:1047–1064. doi:[10.1007/s00382-011-1042-0](https://doi.org/10.1007/s00382-011-1042-0)
- Houtekamer PL, Mitchell HL (2001) A sequential ensemble Kalman filter for atmospheric data assimilation. *Mon Weather Rev* 129:123–137
- Huntley HS, Hakim GJ (2010) Assimilation of time-averaged observations in a quasi-geostrophic atmospheric jet model. *Clim Dyn* 35:995–1009. doi:[10.1007/s00382-009-0714-5](https://doi.org/10.1007/s00382-009-0714-5)
- Keenlyside N, Latif M, Jungclaus J, Kornbluh L, Roeckner E (2008) Advancing decadal-scale climate prediction in the North Atlantic sector. *Nature* 453:84–88
- Knight JR, Allan RJ, Folland CK, Vellinga M, Mann ME (2005) A signature of persistent natural thermohaline circulation cycles in observed climate. *Geophys Res Lett* 32:L020708
- Latif M, Keenlyside NS (2011) A perspective on decadal climate variability and predictability. *Deep-Sea Res II* 58:1880–1894
- Latif M, Roeckner E, Botzet M, Esch M, Haak H, Hagemann S, Jungclaus J, Legutke S, Marsland S, Mikolajewicz U, Mitchell J (2004) Reconstructing, monitoring, and predicting multidecadal-scale changes in the north Atlantic thermohaline circulation with sea surface temperature. *J Clim* 17:1605–1614
- Lorenz EN (1984) Irregularity. A fundamental property of the atmosphere. *Tellus* 36A:98–110
- Matei D, Pohlmann H, Jungclaus JH, Muller WA, Haak H, Marotzke J (2012) Two tales of initializing decadal climate prediction experiments with the ECHAM/MPI-OM model. *J Clim* 25:8502–8523. doi:[10.1175/JCLI-D-11-00633](https://doi.org/10.1175/JCLI-D-11-00633)
- Meehl GA, Teng H (2012) Case studies for initialized decadal hindcasts and predictions for the Pacific region. *Geophys Res Lett* 39:L22705. doi:[10.1029/2012GL053423](https://doi.org/10.1029/2012GL053423)
- Meehl GA, Goddard L, Boer G, Burgman R, Branstator G, Cassou C, Corti S, Danabasoglu G, Doblas-Reyes F, Hawkins E, Karspeck A, Kimoto M, Kumar A, Matei D, Mignot J, Msadek R, Pohlman H, Rienecker M, Rosati T, Schneider E, Smith D, Sutton R, Teng H, van Oldenborgh GJ, Vecchi G, Yeager S (2014) Decadal climate prediction. An update from the trenches. *Bull Am Meteor Soc* 95(2):243–267. doi:[10.1175/BAMS-D-12-00241.1](https://doi.org/10.1175/BAMS-D-12-00241.1)
- Meinville M, Brankart JM, Brasseur P, Barnier B, Dussin R, Verron J (2013) Optimal adjustment of the atmospheric forcing parameters of ocean models using sea surface temperature data assimilation. *Ocean Sci* 9:867–883. doi:[10.5194/os-9-867-2013](https://doi.org/10.5194/os-9-867-2013)
- Mochizuki T, Sugiura N, Awaji T, Toyoda T (2009) Seasonal climate modeling over the Indian Ocean by employing a 4D-VAR coupled data assimilation approach. *J Geophys Res* 114:C11003. doi:[10.1029/2008JC005208](https://doi.org/10.1029/2008JC005208)
- Mochizuki T, Ishii M, Kimoto M, Chikamoto Y, Watanabe M, Nozawa T, Sakamoto TT, Shiogama H, Awaji T, Sugiura N, Toyoda T, Yasunaka S, Tatebe H, Mori M (2010) Pacific decadal oscillation hindcasts relevant to near-term climate prediction. *Proc Nat Acad Sci USA* 107:1833–1837
- Nash J, Sutcliffe J (1970) River flow forecasting through conceptual models. Part I: a discussion of principles. *J Hydrol* 10:282–290
- Oke PR, Allen JS, Miller RN, Egbert GD, Kosro PM (2002) Assimilation of surface velocity data into a primitive equation coastal ocean model. *J Geophys Res* 107(C9):3122. doi:[10.1029/2000JC000511](https://doi.org/10.1029/2000JC000511)
- Oke PR, Schiller A, Griffin DA, Brassington GB (2005) Ensemble data assimilation for an eddy-resolving ocean model of the Australian region. *Q J R Meteor Soc* 131:3301–3311. doi:[10.1256/qj.05.95](https://doi.org/10.1256/qj.05.95)
- Oke PR, Sakov P, Corney SP (2007) Impacts of localisation in the EnKF and EnOI: experiments with a small model. *Ocean Dyn* 57:32–45. doi:[10.1007/s10236-006-0088-8](https://doi.org/10.1007/s10236-006-0088-8)
- Pohlmann H, Jungclaus JH, Köhl A, Stammer D, Marotzke J (2009) Initializing decadal climate predictions with the GECCO oceanic synthesis: effects on the North Atlantic. *J Clim* 22:3926–3938
- Pohlmann H, Müller WA, Kulkarni K, Kameswarrao M, Matei D, Vamborg FSE, Kadow C, Illing S, Marotzke J (2013) Improved forecast skill in the tropics in the new MiKlip decadal climate predictions. *Geophys Res Lett* 40:5798–5802. doi:[10.1002/2013GL058051](https://doi.org/10.1002/2013GL058051)
- Roberts CD, Garry FK, Jackson LC (2013) A multimodel study of sea surface temperature and subsurface density fingerprints of the Atlantic meridional overturning circulation. *J Clim* 26:9155–9174. doi:[10.1175/JCLI-D-12-00762.1](https://doi.org/10.1175/JCLI-D-12-00762.1)
- Robson JI, Sutton RT, Smith DM (2012) Initialized decadal predictions of the rapid warming of the North Atlantic ocean in the mid 1990s. *Geophys Res Lett* 39:L19713. doi:[10.1029/2012GL053370](https://doi.org/10.1029/2012GL053370)
- Roebber PJ (1995) Climate variability in a low-order coupled atmosphere–ocean model. *Tellus* 47A:473–494
- Roemmich D, Johnson GC, Riser S, Davis R, Gilson J, Owens WB, Garzoli SL, Schmid C, Ignaszewski M (2009) The Argo Program: observing the global ocean with profiling floats. *Oceanography* 22(2):34–43. doi:[10.5670/oceanog.2009.36](https://doi.org/10.5670/oceanog.2009.36)
- Shaffrey L, Sutton R (2006) Bjerknes compensation and the decadal variability of the energy transports in a coupled climate model. *J Clim* 19:1167–1181
- Smith GC, Haines K, Kanzow T, Cunningham S (2010) Impact of hydrographic data assimilation on the modelled Atlantic meridional overturning circulation. *Ocean Sci* 6:761–774. doi:[10.5194/os-6-761-2010](https://doi.org/10.5194/os-6-761-2010)
- Smith DM, Scaife AA, Boer GJ, Caian M, Doblas-Reyes FJ, Guémas V, Hawkins E, Hazeleger W, Hermanson L, Ho CK, Ishii M, Kharrin V, Kimoto M, Kirtman B, Lean J, Matei D, Merryfield WJ, Muller WA, Pohlmann H, Rosati A, Wouters B, Wyser K (2013) Real-time multi-model decadal climate predictions. *Clim Dyn* 41:2875–2888. doi:[10.1007/s00382-012-1600-0](https://doi.org/10.1007/s00382-012-1600-0)
- Srokoc M, Baringer M, Bryden H, Cunningham S, Delworth T, Lozier S, Marotzke J, Sutton R (2012) Past, present and future changes in the Atlantic meridional overturning circulation. *Bull Am Meteor Soc* 93(11):1663–1676
- Steiger NJ, Hakim GJ, Stieg EJ, Battisti DS, Roe GH (2014) Assimilation of time-averaged pseudoproxies for climate reconstruction. *J Clim* 27:426–441. doi:[10.1175/JCLI-D-12-00693.1](https://doi.org/10.1175/JCLI-D-12-00693.1)
- Stepanov VN, Haines K, Smith GC (2012) Assimilation of RAPID array observations into an ocean model. *Q J R Meteor Soc* 138:2105–2117. doi:[10.1002/qj.1945](https://doi.org/10.1002/qj.1945)
- Stommel HM (1961) Thermohaline convection with two stable regimes of flow. *Tellus* 13:224–230
- Sugiura N, Awaji T, Masuda S, Mochizuki T, Toyoda T, Miyama T, Igarashi H, Ishikawa Y (2008) Development of a four-dimensional variational coupled data assimilation system for enhanced analysis and prediction of seasonal to interannual climate variations. *J Geophys Res* 113:C10017. doi:[10.1029/2008JC004741](https://doi.org/10.1029/2008JC004741)
- Swingedouw D, Mignot J, Labetoulle S, Guilyardi E, Madec G (2013) Initialisation and predictability of the AMOC over the last 50 years in a climate model. *Clim Dyn* 40:2381–2399. doi:[10.1007/s00382-012-1516-8](https://doi.org/10.1007/s00382-012-1516-8)
- Tardif R, Hakim GJ, Snyder C (2014) Coupled atmosphere–ocean data assimilation experiments with a low-order climate model. *Clim Dyn* 43:1631–1643. doi:[10.1007/s00382-013-1989-0](https://doi.org/10.1007/s00382-013-1989-0)

- Tatebe H, Ishii M, Mochizuki T, Chikamoto Y, Sakamoto TT, Komuro Y, Mori M, Yasunaka S, Watanabe M, Ogochi K, Suzuki T, Nishimura T, Kimoto M (2012) The initialization of the MIROC climate models with hydrographic data assimilation for decadal prediction. *J Meteor Soc Japan* 90A:275–294. doi:[10.2151/jmsj.2012-A14](https://doi.org/10.2151/jmsj.2012-A14)
- Taylor KE, Stouffer RJ, Meehl GA (2012) An overview of CMIP5 and the experiment design. *Bull Am Meteor Soc* 93(4):485–498
- Troccoli A, Palmer TN (2007) Ensemble decadal predictions from analysed initial conditions. *Philos Trans R Soc Lond A* 365:2179–2191
- Wallace J, Lim G, Blackmon M (1988) Relationship between cyclone tracks, anticyclone tracks and baroclinic waveguides. *J Atmos Sci* 45:438–462
- Wang C, Zhang L (2013) Multidecadal ocean temperature and salinity variability in the tropical North Atlantic: linking with the AMO, AMOC, and subtropical cell. *J Clim* 26:6137–6162. doi:[10.1175/JCLI-D-12-00721.1](https://doi.org/10.1175/JCLI-D-12-00721.1)
- Yang X, Rosati A, Zhang S, Delworth TL, Gudgel RG, Zhang R, Vecchi G, Anderson W, Chang YS, DelSole T, Dixon K, Msadek R, Stern WF, Wittenberg A, Zeng F (2013) A predictable AMO-like pattern in GFDLs fully-coupled ensemble initialization and decadal forecasting system. *J Clim* 26:650–661. doi:[10.1175/JCLI-D-12-00231.1](https://doi.org/10.1175/JCLI-D-12-00231.1)
- Yeager S, Karspeck A, Danabasoglu G, Tribbia J, Teng H (2012) A decadal prediction case study: Late twentieth-century North Atlantic ocean heat content. *J Clim* 25:5173–5189. doi:[10.1175/JCLI-D-11-00595.1](https://doi.org/10.1175/JCLI-D-11-00595.1)
- Zhang S, Harrison MJ, Rosati A, Wittenberg A (2007) System design and evaluation of coupled ensemble data assimilation for global oceanic climate studies. *Mon Weather Rev* 135(10):3541–3564
- Zhang S, Rosati A, Delworth T (2010) The adequacy of observing systems in monitoring the Atlantic meridional overturning circulation and North Atlantic climate. *J Clim* 23:5311–5324